Tutor/s

Dra. Teresa Andreu Arbella
Departament de Ciència de Materials i Química Física

Dra. Maria Sarret Pons
Departament de Ciència de Materials i Química Física

Grau de Química

Treball Final de Grau

Chemical etching of layered double hydroxides.
Desaleació química d'hidròxids dobles laminars.

Martí Molera Janer

January 2021

UNIVERSITAT DE BARCELONA

B:KC Barcelona Knowledge Campus
Campus d'Excel·lència Internacional

Electric power is everywhere present in unlimited quantities and can drive the world's machinery without the need for coal, oil or gas or any other of the common fuels.

Nikola Tesla

Vull agrair als meus pares Jordi i Eulàlia i germanes Alba i Mariona tot el suport i ànims que m'han donat, a la Bruna i la Magalí per ser les millors companyes de pis que un pot demanar en aquests moments tan incerts, a la Judit per fer-me companyia durant tots els dinars entre experiments i a les meves fantàstiques tutores Maria i Teresa per la seva increïble implicació i ajuda durant tot el treball.

REPORT

CONTENTS

1. SUMMARY

Layered double hydroxides (LDH) are a family of materials with a variety of uses. Recently nickel based LDH have been studied for its properties as electrocatalysts for the water splitting reaction.

In this work we will study if the addition and the latter removal of aluminium into the LDH structure improves the material properties as oxygen evolution catalyst. The LDH has been synthesized in three different metal combinations (nickel, nickel-iron and nickel-molybdenum) over a nickel foam support with a hydrothermal method. Both the structural and electrochemical properties of the material have been studied. Moreover, we studied an alternative method to deposit the LDH over the support with different grades of success.

In the end, this study shows that only the metal combination of nickel and iron has the potential to become a useful electrocatalyst, and the removal of aluminium from a DLH does not make a better electrocatalyst compared with the non-aluminium counterpart.

Keywords: LDH, hydrothermal method, electrocatalysts, aluminium.

2. RESUM

Els hidròxids doble laminars (LDH) són una família de materials amb molts usos i en els últims anys els LDH de níquel han estat tema d'estudi per les seves propietats com a electrocatalitzadors en la reacció de separació de l'aigua.

En aquest treball estudiarem l'efecte que té la introducció i la posterior eliminació d'alumini a l'estructura d'un LDH i veure si aquest tractament millora les propietats del material com a catalitzador per l'evolució d'oxigen. L'estudi es centrarà en tres combinacions de metalls diferents (níquel, níquel-ferro i níquel-molibdè). El LDH ha estat sintetitzat sobre un suport de níquel porós, o *nickel foam*, amb un mètode de síntesi hidrotermal. S'han estudiat tant les propietats electroquímiques com l'estructura del material. Addicionalment hem estudiat un mètode alternatiu per depositar el LDH sobre el suport, amb diferents grau d'èxit.

En resum, l'estudi mostra que només la combinació de metalls níquel i ferro té potencial per esdevenir un bon electrocatalitzador, i que l'eliminació d'alumini de l'estructura no millora les propietats electrocatalitiques del LDH respecte l'equivalent sense alumini.

Paraules clau: LDH, mètode hidrotermal, electrocatalitzadors, alumini.

3. INTRODUCTION

3.1. WATER SPLITTING REACTION

The water splitting reaction is the process of water decomposition into oxygen and hydrogen, and when electricity is used as the source of energy, it is called water electrolysis.

Oxygen is very abundant in the atmosphere and its production is not a priority. On the other hand, hydrogen is the future for large scale energy storage and can be the solution to the dependence on fossil fuels that our society has now [1]. Studies are focusing on the water splitting electrolysis reaction composed by the oxygen evolution reaction (OER) coupled with the hydrogen electron reaction (HER) given that these half-reactions are the base for large scale hydrogen production as observed in Figure 3.1. Taking the reversible hydrogen electrode (RHE) as a reference these reactions have a thermodynamic potential (E) of 1.23 V *vs* RHE for the OER and 0 V *vs* RHE for the HER.

These reactions however suffer from a lack of efficiency and require electrocatalysts to function [2].

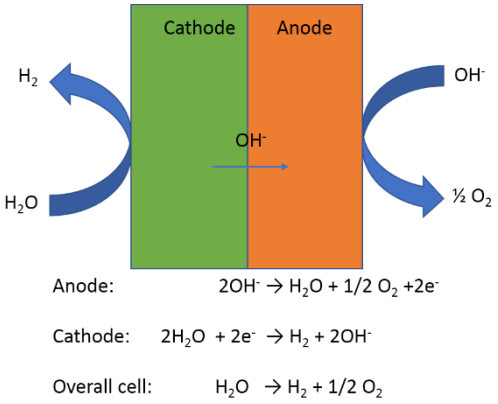

Figure 3.1. Water electrolysis in an alkaline medium.

The OER reaction can happen in any aqueous medium but alkali medium with nickel based electrocatalyst offer the most efficient reaction. In these conditions the OER has a complex

mechanism involving 4 electrons described by the following equations assuming M is a metallic site on the surface [3].

$$M + OH^- \rightleftharpoons MOH + e^- \quad (1)$$

$$MOH + OH^- \rightleftharpoons MO + H_2O + e^- \quad (2)$$

$$MO + OH^- \rightleftharpoons MOOH + e^- \quad (3)$$

$$MOOH + OH^- \rightleftharpoons MOO^- + H_2O \quad (4)$$

$$MOO^- \rightleftharpoons M + O_2 + e^- \quad (5)$$

3.2. LAYERED DOUBLE HYDROXIDES

Layered double hydroxides (LDH) are a family of materials who share a structure composed of brucite-like metal hydroxide layers with intercalated anions [4]. As seen in Figure 3.2 the metals are in two different oxidation states M^{2+} and M^{3+} surrounded by hydroxide ions forming the hydroxide layer, and between these layers there are anions to compensate the charge and water.

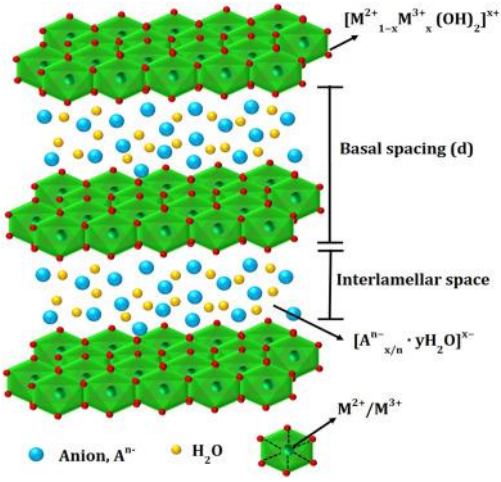

Figure 3.2. Detailed LDH structure [5].

LDH lately have emerged as an alternative to noble metals catalysts for the water splitting reaction [6] among other applications such as energy storage in the form of supercapacitors [7] or catalysis [8].

To synthesize these materials there are various methods, electrochemical deposition [9], hydrothermal [10], coprecipitation [11] and ion-exchange [5] being some of them.

In this work we will be focusing on the hydrothermal synthesis with urea decomposition because it shows great promise to obtain the material over various supports achieving a more crystalline solid than other methods.

This method consists of a synthesis in an autoclave in high temperature and pressure conditions, with a slow increase in basicity given by urea decomposition at high temperatures [12].

3.3. OVERPOTENTIAL (η)

Overpotential (η) is the difference between the thermodynamic potential of the reaction and the one applied to achieve a given current density. There are a lot of causes for an overpotential to occur thus, there are several factors that contribute to this increment. A concentration gradient (mass transport), an electrochemical reaction (charge transfer) or having an internal electrical resistance (ohmic drop) are some of the most common causes for an overpotential.

When a reaction is happening around an electrode if the rate of reaction is higher than the diffusion velocity of the reagents a diffusion layer is created and an overpotential due to mass transport is needed to carry the reagents to the electrode.

An ohmic drop overpotential appears in high intensity currents and it depends on the resistance and intensity of the current [13].

When an electrochemical reaction is happening, for kinetic reasons an overpotential appears to overcome the activation energy of the charge transfer and the only way to reduce it is with the adequate catalyst. Then, the current density is related with the overpotential by the Butler-Volmer equation (Equation 6) and any experiment involving charge transfer must take that into account.

$$j = j_0 * \left\{ e^{\left(\frac{\beta_a Z F}{RT}\eta\right)} - e^{\left(-\frac{\beta_c Z F}{RT}\eta\right)} \right\} \quad (6)$$

In this work, we will be focused in the overpotential due to the chemical reaction; so the other overpotentials will have to be taken into consideration and corrected if necessary.

When the overpotential of the Butler-Volmer equation is highly positive the anodic component of the equation dominates and the cathodic part is negligible, and vice versa when the overpotential is negative. These simplifications are known as the Tafel equations and their slope (A) gives useful information about the limiting step of the reaction's mechanism, and are described by the next equations (Equation 7 for positive overpotential and Equation 8 for negative overpotential).

$$\eta = A \cdot \log_{10} j \ + c_a \quad (7)$$

$$\eta = -A \cdot \log_{10} j \ + c_c \quad (8)$$

4. OBJECTIVES

The main objective in this work is to evaluate the effects of adding aluminium into the Ni, NiFe and NiMo LDH electrocatalysts for the water splitting reaction and improve it through chemical and electrochemical treatments to create defects in its structure.

To achieve this aim, the following objectives have been summarized:

- Synthesis of different electrodes with 3 different metal combinations (NiAl, NiFeAl and NiMoAl) and its non-aluminium counterparts (Ni, NiFe, NiMo) via a hydrothermal method on NF substrates.

- Modification of the electrodes with chemical etching (CHE) and electrochemical etching (ECE) treatments.

- Study of the material deposited in the support with various characterization techniques.

-Measurement of different electrodes as electrocatalysts towards the OER.

-Evaluate the preparation of electrodes via ink deposition of LDH powders.

5. EXPERIMENTAL SECTION

5.1 REAGENTS

In this work we used the following list of reagents to synthesise the LDH samples and its characteristics are summarized in Table 5.1.

Table 5.1. List of reagents

reagent	purity [%]	Provider
$Ni(NO_3)_2{\cdot}6H_2O$	≥99.4	JT Baker
$Al(NO_3)_3{\cdot}9H_2O$	≥98	Sigma-Aldrich
$FeSO_4{\cdot}7H_2O$	≥99.5	Merck
$Na_2MoO_4{\cdot}2H_2O$	≥99.5	Merck
CH_4N_2O (Urea)	≥99.5	Merck

5.2 SYNTHESIS

First, we cleaned the nickel foam (NF) in an ultrasonic bath, first with acetone and then with HCl 6M solution, for 2 minutes each. Afterwards we dried and weighted them.

We prepared a solution consisting of different metals and urea with a total metal concentration of approximately 0.15M (see Table 5.2). Sample names indicate the metals used in their synthesis (ex. a sample synthesised in a nickel and aluminium solution is called NiAl). For each solution we made 3 samples, to differentiate them we cut 1 corner in one and 2 in another calling them by the number of cut corners like in Figure 5.1.

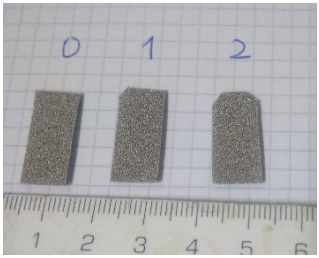

Figure 5.1. Nickel foam support

Table 5.2. Concentration of the different metal solutions.

Sample	Ni^{2+}[M]	Al^{3+}[M]	Mo^{7+}[M]	Fe^{2+}[M]	urea[M]
NiAl	0.111	0.037	–	–	0.530
Ni	0.150	–	–	–	0.517
NiMoAl	0.059	0.038	0.054	–	0.572
NiMo	0.076	–	0.075	–	0.513
NiFeAl	0.056	0.038	–	0.058	0.523
NiFe	0.074	–	–	0.074	0.523

Then, we poured the metal solution into the Teflon container of the autoclave (Figure 5.2), added the NF electrodes (cleaned and weighted), sealed it and put it into the oven at 120ºC during 12h. The initial pH of the solution is acidic around 3, but when the urea decomposes thermally to ammonium hydroxide and hydrogen carbonate the solution becomes alkaline with a pH around 10. This basicity causes the precipitation of the metals as LDH onto the NF electrode or as particles in suspension.

Then, once the autoclave has cooled, we clean the electrodes with deionized water and once they have dried, we weight them. The solid residue that's left in the Teflon container is filtered in a number 3 filter plate.

Figure 5.2. Autoclave container with all the pieces (left) and assembled (right).

Some of the prepared electrodes received a chemical etching treatment in which they were immersed in a 6M KOH solution for 1 hour or an electrochemical etching treatment in which they were soaked in a 1M KOH solution during 20 hours with a 0.369 V *vs* RHE applied potential [2].

These treatments are made to change the structure of the deposited material and see if it improves the material qualities.

Another method we tried to make the LDH electrodes was ink deposition [13]. This method consisted of mixing 10 mg of the hydrothermal synthesised LDH with 86,6 µg of Nafion117 and 1 ml of ethanol, then the mixture was left in an ultrasonic bath for 30 minutes. Finally, the solution was added to a 1 cm^2 NF electrode.

Five samples were made with this method, but there were small differences in the preparation of each sample as summarized in Table 5.3:

-In some samples the electrode was heated before the deposition.

-In some samples the quantity deposited was doubled.

-In some samples the Nafion177 was not added.

Table 5.3. Characteristics of ink deposition samples.

Sample	Temperature	Quantity deposited (µl)	Nafion177
NNiFe 1	Cold	167	Yes
NNiFe 2	Hot	167	Yes
NNiFeAl	Hot	167	Yes
NNiFe 3	Cold	334	Yes
NNiFe 4	Cold	167	No

5.3 MATERIAL CHARACTERIZATION

To know about the sample composition, we made a scanning electron microscopy (SEM) coupled with an energy dispersive X-ray spectroscopy (EDX) measure with a Quanta 200 microscope to see the morphology of the deposited LDH and its atomic composition. We only made the characterization for samples without a chemical etching treatment.

As we did not want any modifications to the sample we chose the ones that had not been through the electrochemical tests, since the samples turn black after the measures.

We also did an attenuated total reflection (ATR) with a PerkinElmer FT-IR spectrometer Spectrum Two to characterize the solid residue of the synthesis. In this case we analysed the normal solid residue, but also a chemically treated one to have a better idea of the consequences

of the treatment in the material.

The last test we did regarding the material composition was an X-ray diffraction (XRD) with a Siemens D500 diffractometer to know about the crystallinity of the deposited material, and to further confirm that the material is indeed an LDH. This test was only done to the iron samples. These measurements were performed in the Centres Científico Tècnics of the University of Barcelona (CCiT UB).

5.4 ELECTROCHEMICAL CHARACTERIZATION

To make the electrochemical measures we used a VSP-3 potentiostat from Biologic and the program EC-Lab V11.31 to make the data interpretation.

As said in the introduction measuring the correct overpotential is essential for a good characterization, so an ohmic drop correction for the overpotential due to the resistance of the circuit is needed. With the EC-Lab program we corrected the ohmic drop with the ZIR technique that measures the resistance of the circuit, and with Ohm's law [13] compensating 95% of the resistance R given an intensity I following the next formula.

$$E = E_{aplied} - 95\%IR \quad (7)$$

The other possible cause for unwanted overpotential is the formation of a diffusion layer, but this should not be a problem with the high OH^- concentration from the alkali KOH medium.

To measure the material response to a determined voltage we made some electrochemical measures. All measures were made in a three electrodes cell with the sample functioning as the working electrode (WE), a platinum electrode as the counter electrode (CE) and a saturated calomel electrode (SCE) or a silver/silver chloride electrode 3.5M (Ag/AgCl) as the reference electrode (RE) in a KOH 1M electrolyte as seen in Figure 5.3. Since all the measures are converted to RHE the one used in each sample is irrelevant [6].

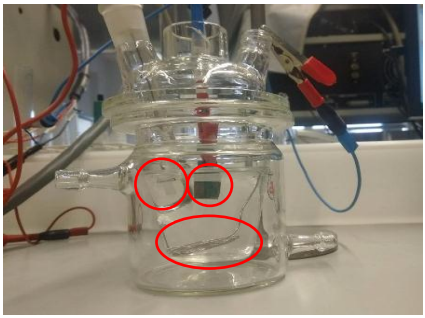

Figure 5.3. Electrolytic cell with CE (right/bottom), WE (middle), RE (left).

There are different measures made for each sample:

- First, we start with a rest potential for 15 minutes to stabilize the sample.

- Then we make a cyclic voltammetry between a range of 0.77 V to 1.87 V *vs* RHE for 10 cycles with a scan rate of 20 $mV \cdot s^{-1}$ to know about the different oxidation and reduction processes in the sample.

- A polarization curve or linear sweep voltammetry (LSV) is measured with a range from 0.77 V to 1.87 V *vs* RHE at a scan rate of 2$mV \cdot s^{-1}$ This measure is made 2 times one before and one after the ohmic drop correction.

- Then the LSV measures are repeated in a smaller potential range and a much slower velocity to get the start of the OER curve to be able to determine the Tafel slopes. This LSV is done in a 0.2 V range in a velocity of 0.166 $mV \cdot s^{-1}$ between 1.37 and 1.57 V *vs* RHE but in some samples this interval can change, since the interval is determined from the previous LSV. Also, as the previous LSV this one is done before and after the ohmic drop correction.

6. NICKEL SAMPLES

Different characterization techniques have been done to measure the properties of the samples. To determine the interlayer anions in the sample an ATR has been done and a SEM-EDX gave information of the deposition and the atomic composition. The cyclic voltammetry shows the redox processes of the sample, the polarization curves quantify the overpotential of the OER reaction and the Tafel slopes determine the mechanism.

6.1 MATERIAL CHARACTERIZATION

The ATR analysis of all samples and precursors (Figure 6.1) gives crucial information about the composition of the interlayer of anions present in the LDH. The wide band in the 3400 cm^{-1} region is due to water and hydroxide molecules [14]. At 1300 cm^{-1} there is a peak corresponding to nitrate anions [14]. Some compounds show a band at about 1600cm^{-1} [14] corresponding to ammonia and below 1000cm^{-1} it's the footprint region and is different in each compound. Thanks to these differences we can know that adding aluminium changes the obtained LDH.

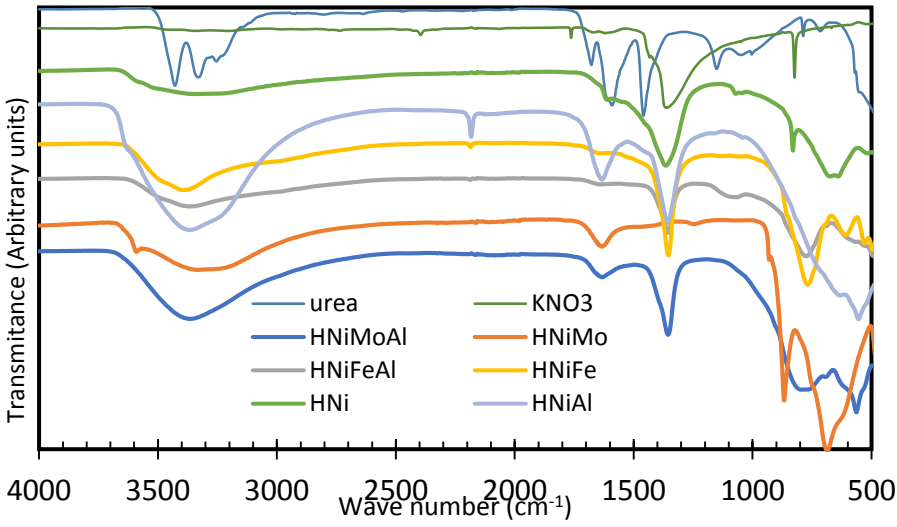

Figure 6.1. ATR peaks for all samples.

In Figure 6.2, it is compared the samples Ni and NiAl as synthesised and after chemical etching. As it can be seen, Ni samples do not have a high concentration of interlayer water, and after the chemical etching treatment all water is eliminated (region around 3400 cm^{-1}). In this sample the ammonia, nitrate and hydroxide levels also diminish. The same trend can be observed with the NiAl samples except with the hydroxides, because without the water its peak is clearer. The footprint region, below 1000 cm^{-1} shows that the Ni and the NiAl samples are different in composition.

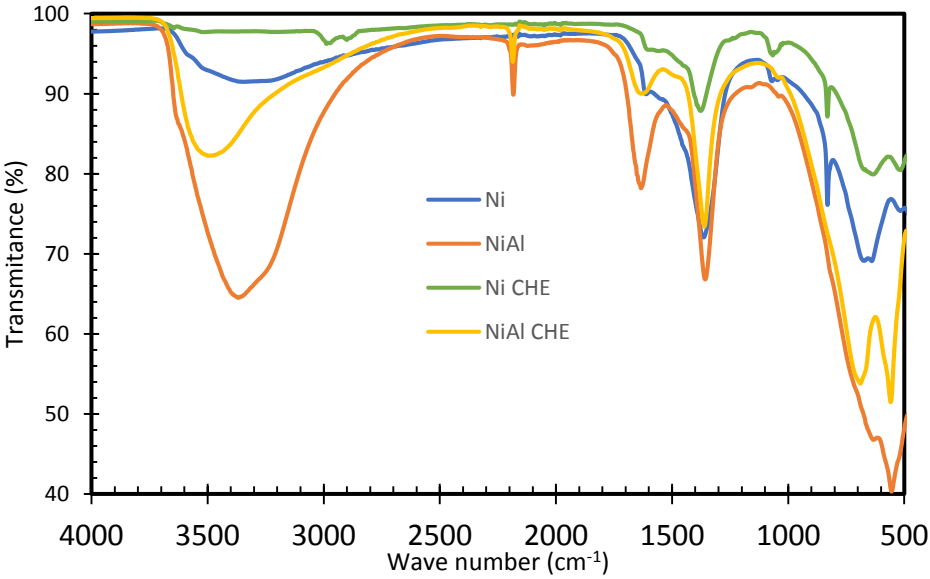

Figure 6.2. ATR peaks of nickel samples.

SEM-EDX analysis from Figure 6.3 show a very low deposition in the Ni sample, whereas the NiAl sample show a laminar deposition and has a much better surface coverage.

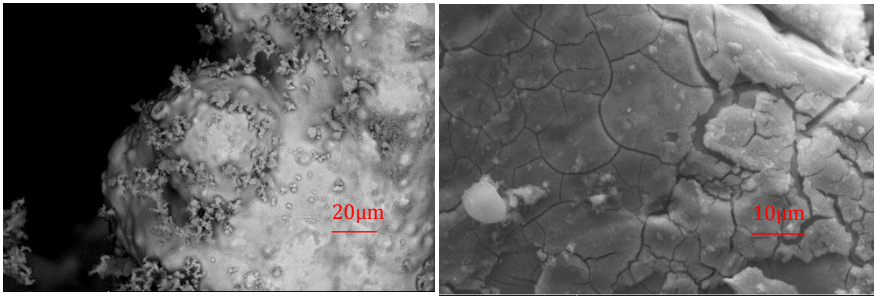

Figure 6.3. LDH deposited to NF support (Ni left and NiAl right).

In Table 6.1 we can see the atomic composition of the deposited LDH and with that information an approximated chemical formula can be deduced, but since the metals can have two different oxidation states the global charge will not be considered. The specific interlayer anion composition won't be discussed either, as no information about it is provided in the analysis.

Oxygen percentage doubles nickel quantities in Ni 2 but is only 12% higher in Ni 1. A $Ni(OH)_2$ formula makes more sense because the Ni 1 sample can be explained if there is a hydroxide deficiency in this point. The Ni samples have minor potassium and aluminium impurities, and a major carbon one but since the sample was coated in carbon that one is not relevant.

In both NiAl samples, oxygen stays in a 2:1 relation with nickel and aluminium combined. This gives a chemical formula of $Ni_xAl_{1-x}(OH)_2$. The nickel and aluminium relation is unknown because in the two analysed points the quantities of both are very different.

Table 6.1. Atomic composition of the LDH nickel samples obtained by EDS.

Sample	Ni (%)	Al (%)	O (%)	S (%)	K (%)	C (%)
Ni 1	40.39	0.22	52.31	-	0.26	6.82
Ni 2	31.85	0.27	60.99	-	0.24	6.65
NiAl 1	31.69	2.04	65.95	0.32	-	-
NiAl 2	22.94	6.92	69.50	0.64	-	-

6.2 ELECTROCHEMICAL CHARACTERIZATION

The cyclic voltammetries in Figure 6.4 show two redox processes. The peak and the valley around 1.25 V vs RHE correspond to the oxidation and reduction of the nickel species in the LDH to NiOOH [6] following the reaction:

$$(\mathrm{NiOH})_2 + \mathrm{OH}^- \rightarrow \mathrm{NiOOH} + \mathrm{H_2O} + \mathrm{e}^- \quad (9)$$

This reaction is irreversible because the two peaks are not symmetric.

In the NiAl sample the oxidation peak is stretched due to the aluminium present in the LDH. Following the peak there is an intensity increase corresponding to the OER reaction electrocatalized by the previously formed NiOOH.

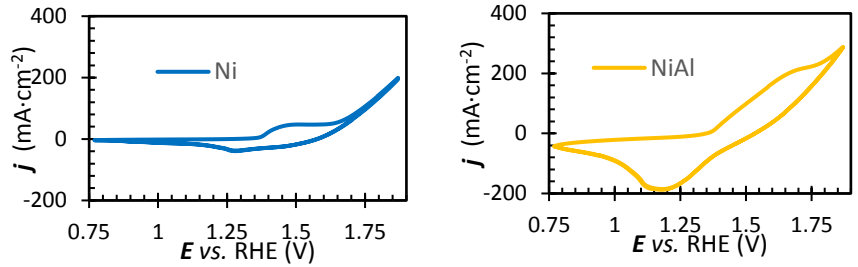

Figure 6.4. Cyclic voltammetry of Ni and NiAl samples at a scan rate of 20 mV·s^{-1}.

To be able to compare the different measurements we normalized them by the quantity of LDH material deposited in the electrode instead of the submerged surface, obtaining the current density *j* in mA·g^{-1} instead of mA·cm^{-2} given by the electrode measured geometric surface.

In Figure 6.5 we can see that Ni samples have a lower overpotential than NiAl samples, meaning that less energy is required to produce the same amount of hydrogen, thus improving the material usefulness. With that said there is not much difference between CHE treated sample and the non-treated ones concluding that the treatment does not have much of an effect. The NiAl samples show an improvement in the ECE treatment, even though the samples do not give better results than the NF blank. Possibly a longer treatment or doing it at a higher potential could make the NiAl samples better than their Ni counterparts.

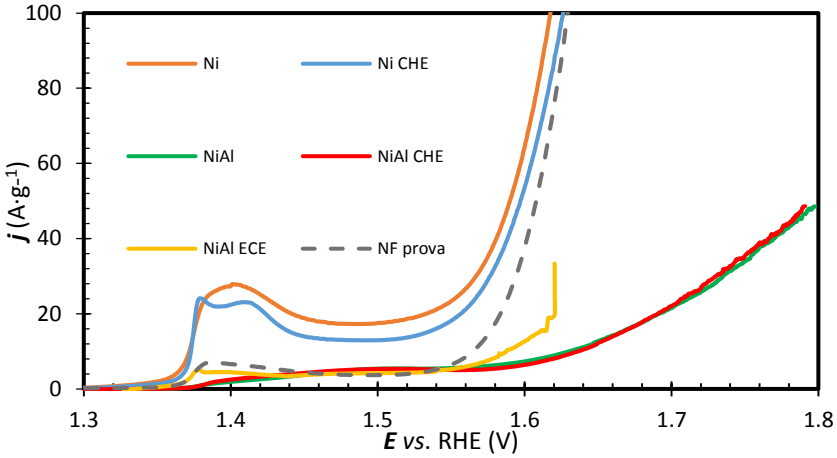

Figure 6.5. Polarization curves of Ni and NiAl samples at a scan rate of 2 mV·s^{-1}.

The overpotentials at Table 6.2 conclude that Ni samples have a smaller overpotential than NiAl samples regardless of the treatment applied to each sample. Also comparing the samples to the NF LSV show that only Ni samples perform slightly better than the NF blank.

Table 6.2. Overpotential of nickel samples at 20 A·g^{-1}.

Sample	η_{20}(mV)	Sample	η_{20} (mV)
Ni	303±6	NiAl	462±6
Ni CHE	327±6	NiAl CHE	461±6
NF	354±6	NiAl ECE	391±6

To determine which step of the mechanism is the limiting step we looked at the Tafel slopes and correlated them with those of bibliography [3].

In the Tafel graphs there is a little superposition between the OER reaction and the oxidation of nickel. Because of that, some mechanisms are overshadowed by the nickel oxidation, and the slope taken to know the mechanism has to be observed at higher intensities.

In the case of Ni samples, the first slope is of 70 mV·dec^{-1} [3] and most closely fits the model where the slope increases until 120 mV·dec^{-1} passing through a region of 60 mV·dec^{-1} [3] corresponding with equation 4 being the limiting step.

For NiAl samples the slope it's close to 120 mV·dec^{-1} [3] from the beginning, thus having equation 1 as the limiting step.

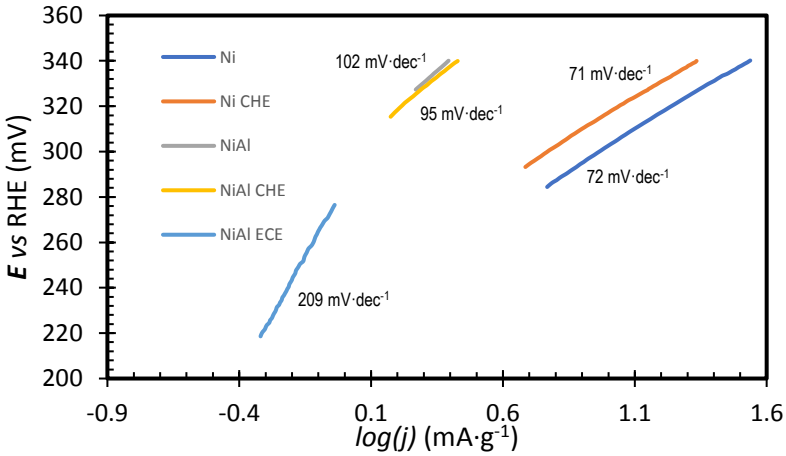

Figure 6.6. Tafel slopes for nickel samples.

7. NICKEL-IRON SAMPLES

Nickel-Iron samples received the same treatments and characterization techniques as the nickel ones in addition to XRD, and due to the overall better results more diverse samples were analysed.

7.1 MATERIAL CHARACTERIZATION

In Figure 7.1 we can see that with a CHE treatment iron samples reduce their water, hydroxide and nitrate amount, but no other changes are appreciable. The NiFeAl samples do not experiment a change at all but that can be attributed to the non-treated sample already having the levels of counter anions in its interlayer at the same levels as the treated nickel-iron NiFe sample.

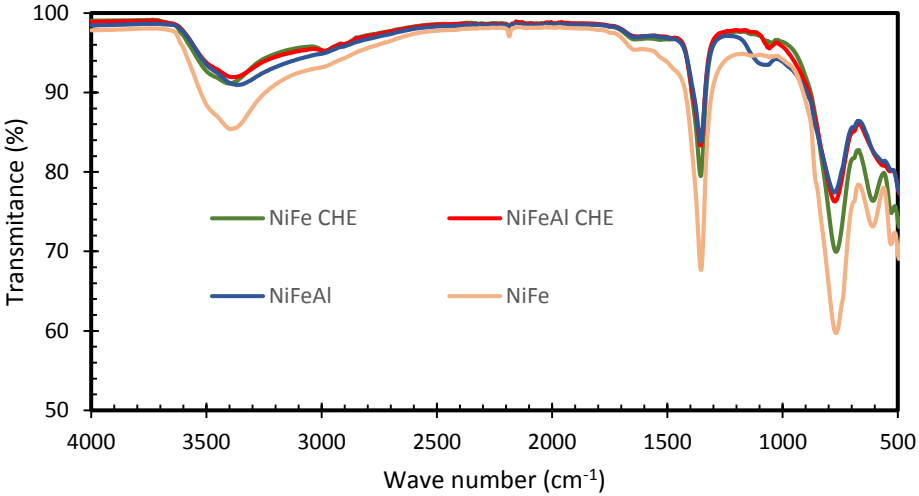

Figure 7.1. ATR peaks for iron samples.

With SEM-EDS we obtained images of the deposition of the LDH to the NF support. In Figure 7.2 we can see that the NiFe sample consists of an array of filaments that grow on the surface whereas the NiFeAl sample has a laminar deposition with little spheres deposited over this laminar base.

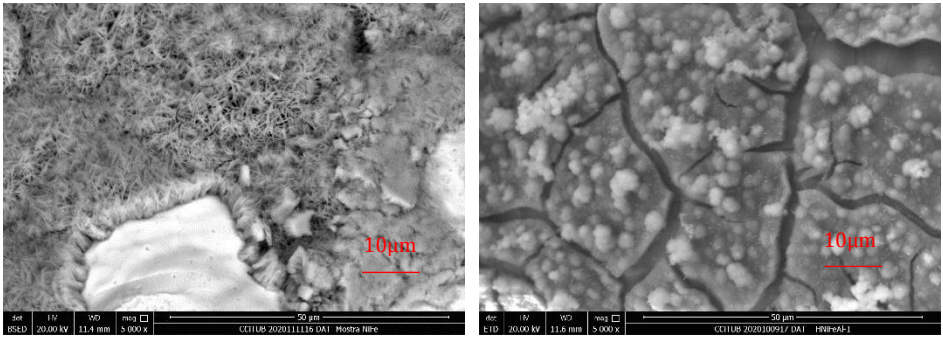

Figure 7.2 SEM micrographs of LDH deposited on NF support (NiFe left and NiFeAl right).

In Table 7.1 NiFe 1 sample has a higher nickel percentage than iron but that could be a local irregularity because in the NiFe 2 sample there is more iron percentage than nickel. If we assume an even quantity of nickel and iron and a 60% of oxygen from the hydroxide, we obtain a formula of $Ni_{0.5}Fe_{0.5}(OH)_2$ for the LDH.

For the NiFeAl samples nickel doubles the iron quantity at least and is even with the aluminium percentage. Assuming a 5% of iron a 10% of nickel and aluminium and the rest being oxygen the LDH formula is $Ni_{0.4}Fe_{0.2}Al_{0.4}(OH)_2$.

Both samples have sulphur impurities, probably from the iron sulphate used in the synthesis.

Table 7.1. Atomic composition of the LDH iron samples obtained by EDS.

Sample	Ni (%)	Fe (%)	Al (%)	O (%)	S (%)	C (%)
NiFe 1	24.86	15.70	0.30	57.58	0.20	1.36
NiFe 2	14.50	16.16	1.40	63.99	0.38	3.57
NiFeAl 1	13.33	4.60	10.32	70.04	1.60	-
NiFeAl 2	8.24	3.89	12.95	73.73	1.20	-

The eight peaks from the Ni LDH JCPDS (38-0715) card correspond to the eight dotted peaks in Figure 7.3, confirming that we have a LDH with a nickel structure after the hydrothermal method. With that said, the peaks are slightly distorted and do not appear at the exact angle because even though iron and nickel atoms have a similar radius the inclusion of iron atoms still makes small changes to the cell parameters. The observed peaks are broad, due to a nanometric size of the crystals. Also, there is a high peak at an angle of 52 and other smaller ones that correspond to metal hydroxycarbonates from the JCPDS cards 83-1764 and 26-1286, but no peak corresponds to aluminium hydroxide concluding that all aluminium is introduced into the material as LDH. Between NiFe and NiFeAl the only major difference is the peak intensity, making it difficult to differentiate between the two.

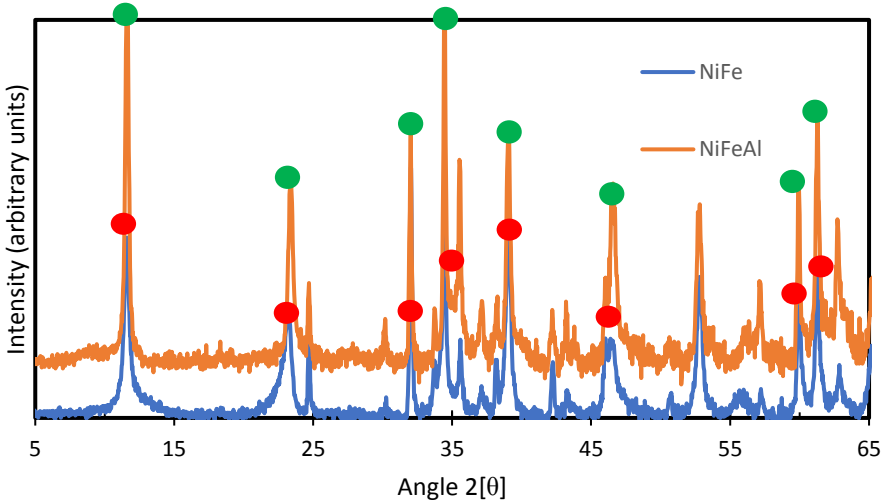

Figure 7.3. X-ray diffractograms corresponding to NiFe and NiFeAl powder particles. Dots correspond to JCPDS 38-0715 (LDH structure).

In figure 7.4 the peaks from JCPDS card also appear, except that around 33º, meaning that this orientation is lacking in the analysed sample. This DRX was done to see changes in the structure derived from the ECE treatment, but the two diffraction patterns are the same, so no changes are perceptible.

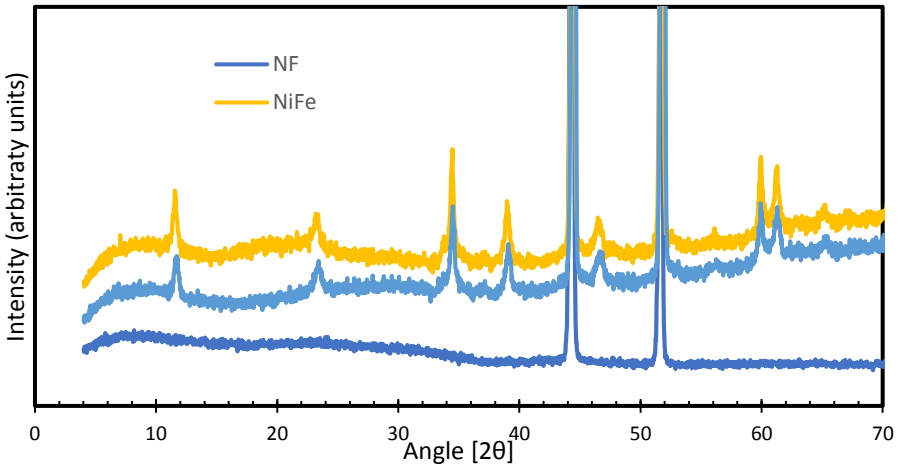

Figure 7.4. X-ray diffractograms corresponding to NiFe LDH deposited over NF.

7.2 ELECTROCHEMICAL CHARACTERIZATION

Figure 7.5 shows the cyclic voltammetries of the nickel-iron samples; they are similar to those of nickel (Figure 6.4), but these peaks might also have iron redox contribution, since iron like nickel can exist in both 2 and 3 oxidation states.

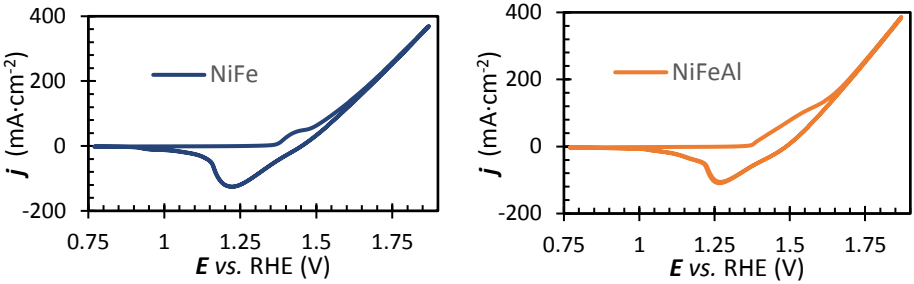

Figure 7.5. Cyclic voltammetry of NiFe and NiFeAl samples with a sweep velocity of 20 mV·s^{-1}.

As can be seen in Figure 7.6 the NiFe samples even though they received different treatments do not show much difference in the exhibited LSV until high current densities. The main difference is that two samples show a different slope than the other three, that can be attributed to the two batches of synthesis resulting in a different LDH distribution. In Table 7.2 can be seen that the overpotential at 20 A·g^{-1} is around 265 mV in all the samples showing that the treatments do not work in a sample without aluminium.

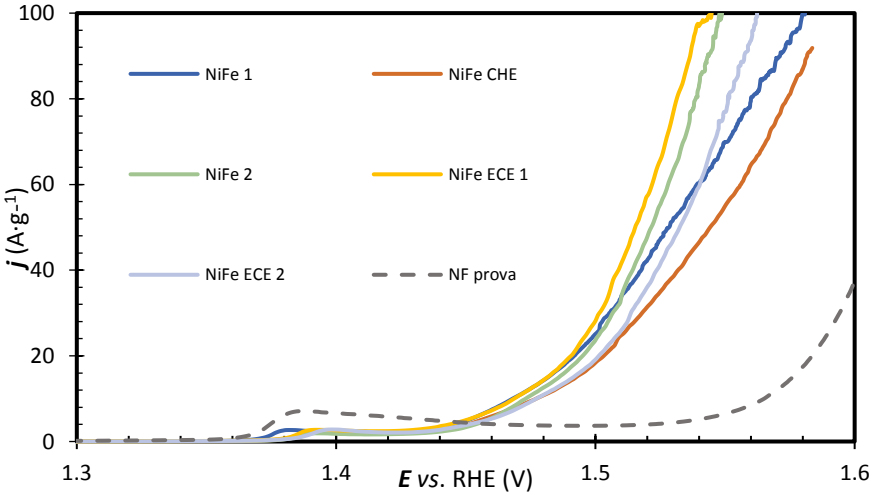

Figure 7.6. Polarization curves of the NiFe samples after different treatments.

Table 7.2. Overpotential of iron samples at 20 $A \cdot g^{-1}$.

Sample	η_{20}(mV)	Sample	η_{20} (mV)
NiFe 1	262±6	NiFeAl 1	328±6
NiFe CHE	274±6	NiFeAl CHE	328±6
NiFe 2	266±6	NiFeAl 2	318±6
NiFe ECE 1	261±6	NiFeAl ECE 1	286±6
NiFe ECE 2	272±6	NiFeAl ECE 2	301±6

The LSV curves of NiFeAl samples in Figure 7.7 show important differences resulting in an average gap of 30 mV between the ECE treated samples and the non-treated ones (Table 7.2). The NiFeAl samples like the previous ones show a different slope depending on the synthesis batch they correspond.

The electrochemical etching process shows a small change in the overpotential but the charge that passed through the two samples is different being 213 $C \cdot g^{-1}$ for NiFeAl ECE 1 and 144 $C \cdot g^{-1}$ for NiFeAl ECE 2. This small change in the total charge of the process can be the cause for the 15 mV difference in the two ECE samples.

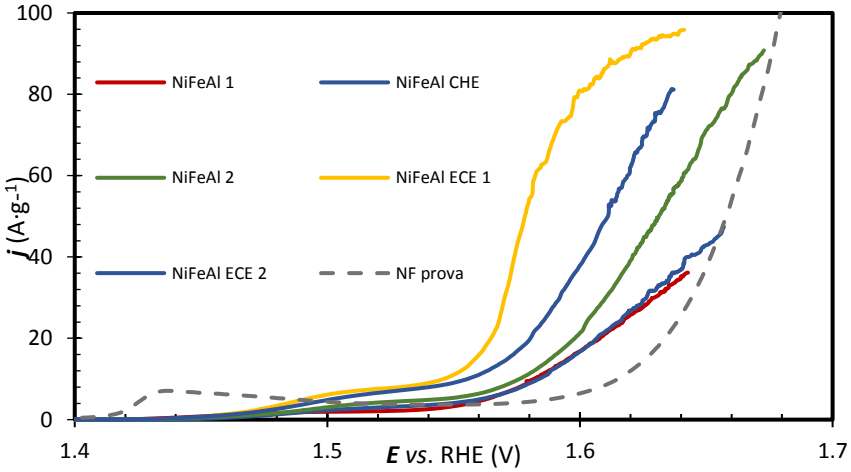

Figure 7.7. Polarization curves of NiFeAl samples after different treatments.

When calculating the limiting step for iron samples a problem emerges because the slopes could belong to two different theoretical models and the only difference is if there is a previous smaller slope or not.

For the NiFe samples in Figure 7.8 the measured slope is 30 mV·dec^{-1} [3] and the two possible limiting steps are equations 2 and 4. In Figure 7.9 NiFeAl samples measured slope is 50 mV·dec^{-1} [3] but in some samples it's a little bit smaller, meaning that these samples could have equations 3 and 5 as their limiting step.

In both the nickel and iron samples the limiting step of the reaction changes between metal compositions, meaning that there is a clear involvement of the LDH in the reaction. It is also important to notice that the samples that received an ECE treatment have the same limiting step as the samples with its equal metal combination concluding that the ECE process does not remove completely the aluminium in the electrode.

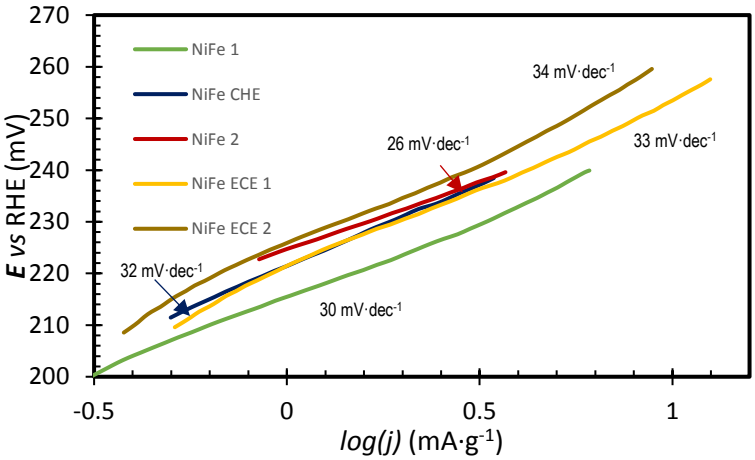

Figure 7.8. Tafel slopes for nickel-iron samples.

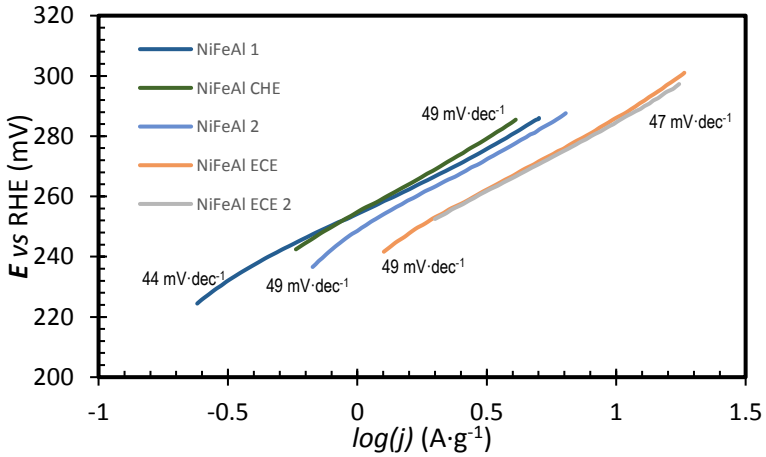

Figure 7.9. Tafel slopes for nickel-iron-aluminium samples.

8. NICKEL-MOLYBDENUM SAMPLES

Nickel-molybdenum samples were originally prepared with the cathodic HER reaction in mind, but due to the results form [15] that idea was scraped and were only used for the OER as the other metal combinations.

In the preparation of molybdenum samples, not a lot of material was deposited, and the standardization for this samples had to be done with the area measured instead of the quantity of material deposited.

8.1 MATERIAL CHARACTERIZATION

The ATR graphs in Figure 8.1 show that in molybdenum samples the CHE treatment reduces water and ammonia content, and as all the other samples the footprint region shows the successful introduction of aluminium in the LDH.

The NiMo powder has an irregularity regarding the nitrate peak, because it does not appear. With that said more data is needed before drawing any conclusion.

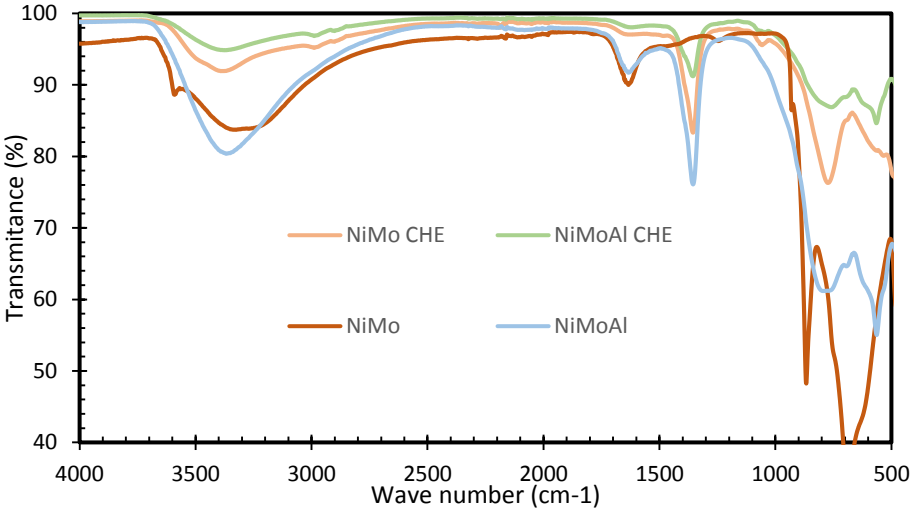

Figure 8.1. ATR peaks for molybdenum samples.

In figure 8.2 we can see that NiMo LDH deposited in a laminar manner with extra material deposited unevenly over, but the NiMoAl only had an uneven and scarce deposition.

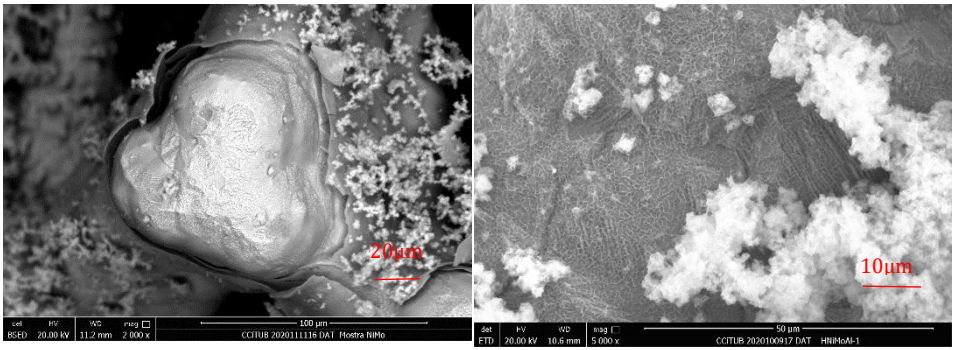

Figure 8.2. LDH deposited to NF support (NiMo left and NiMoAl right).

As summarized in Table 8.1 in NiMo samples there is much more nickel than molybdenum and its combined metal percentage is doubled by the oxygen content, hence corresponding to the formula $Ni_{0.89}Mo_{0.11}(OH)_2$.

In NiMoAl samples the metal-oxygen relation is the same as the NiMo sample, but the quantity of nickel is diminished due to an increase of aluminum, obtaining the chemical formula $Ni_{0.7}Mo_{0.16}Al_{0.13}(OH)_2$.

Table 8.1. Atomic composition of the LDH molybdenum samples.

Sample	Ni (%)	Mo (%)	Al (%)	O (%)	C (%)
NiMo 1	31.66	3.41	0.39	59.53	5.01
NiMo 2	30.91	4.31	0.31	57.94	6.52
NiMoAl 2	23.43	5.36	4.28	66.94	-

8.2 ELECTROCHEMICAL CHARACTERIZATION

In molybdenum samples the redox processes observed in Figure 8.3 are the same as the ones from nickel and iron samples.

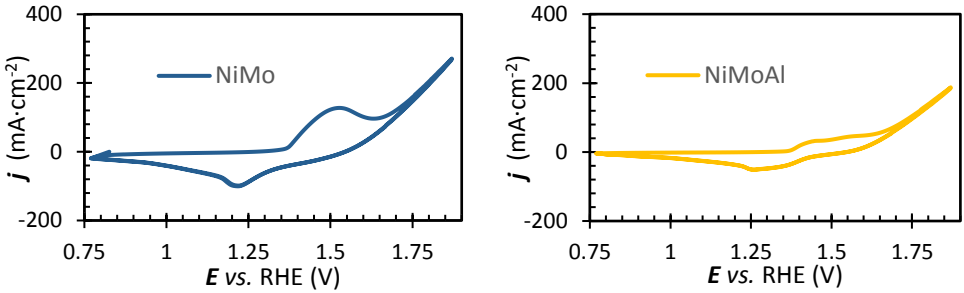

Figure 8.3. Cyclic voltammetry of molybdenum samples at a scan rate of 20 $mV \cdot s^{-1}$.

In Figure 8.4 the LSV curves of molybdenum samples like all the previous electrodes show better overpotentials without aluminium in the mix. In the case of both molybdenum samples the CHE treatment shows a better overpotential at Table 8.2, but the difference is so minimal that it could not be significant enough.

In conclusion, all the NiMo and NiMoAl samples do not have great overpotentials and do not show much promise for future research.

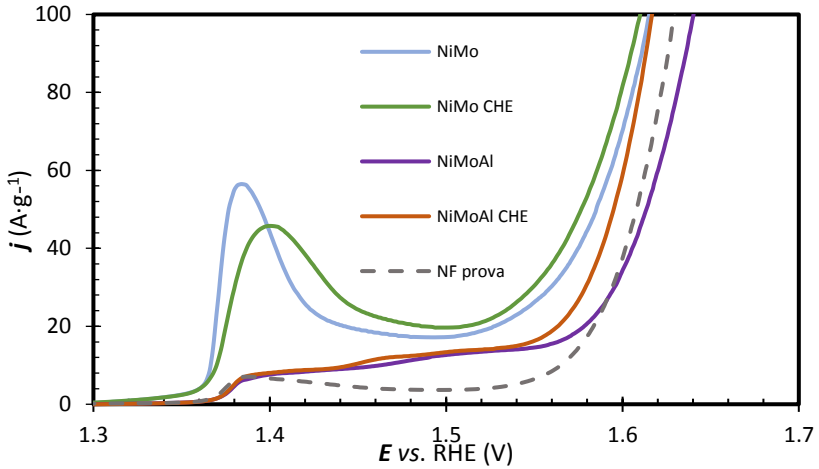

Figure 8.4. Polarization curves of molybdenum samples at a scan rate of 2 $mV \cdot s^{-1}$.

Table 8.2. Overpotential of molybdenum samples at 20 A·cm^{-2}.

Sample	η_{20}(mV)	Sample	η_{20} (mV)
NiMo	301±6	NiMoAl	349±6
NiMo CHE	285±6	NiMoAl CHE	334±6

In Figure 8.5 nickel-molybdenum samples have similar Tafel slopes as the nickel samples, so they have the same limiting step. Equation 1 for NiMo samples and equation 4 for NiMoAl samples. These same results could be because of the low quantity of molybdenum incorporated in the LDH making it function like the nickel samples.

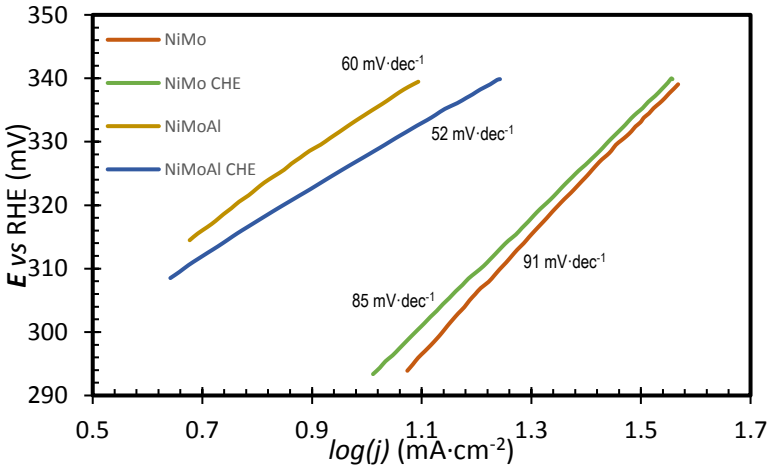

Figure 8.5. Tafel slopes for nickel-molybdenum samples.

9. INK DEPOSITION SAMPLES

Ink deposition samples were few and did not gave impressive results. That being said, it's a more controllable way to deposit the LDH into the NF support and other mixtures can give better performances.

9.1 ELECTROCHEMICAL CHARACTERIZATION

In figure 9.1 we can see that ink deposition samples synthesized in heated NF do not have the oxidation peaks and valleys and the cold samples do, albeit they are smaller in comparison with the hydrothermal method ones. That means this method does not deposit as much material as the hydrothermal method.

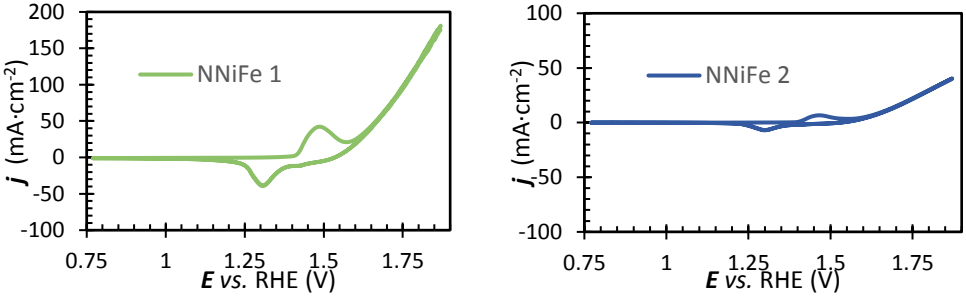

Figure 9.1. Cyclic voltammetry of ink deposition samples with at a scan rate of 20 $mV \cdot s^{-1}$.

In Figure 9.2 the heated samples show overpotentials much worse than the NF blank, meaning that the heat hinders the natural electrochemical properties of the LDH and the substrate. Moreover, doubling the amount of deposited material also hinders the electrode functionality, but that could be because the adding of the LDH was made in two different additions of the 167 µl, so a direct pouring of a more concentrated solution should be made before drawing that conclusion.

Regardless, the sample without Nafion177 is the best of the bunch, with the overpotential from Table 8.2 being a little higher than the one of nickel-iron samples, and with more research this method could substitute the hydrothermal synthesis.

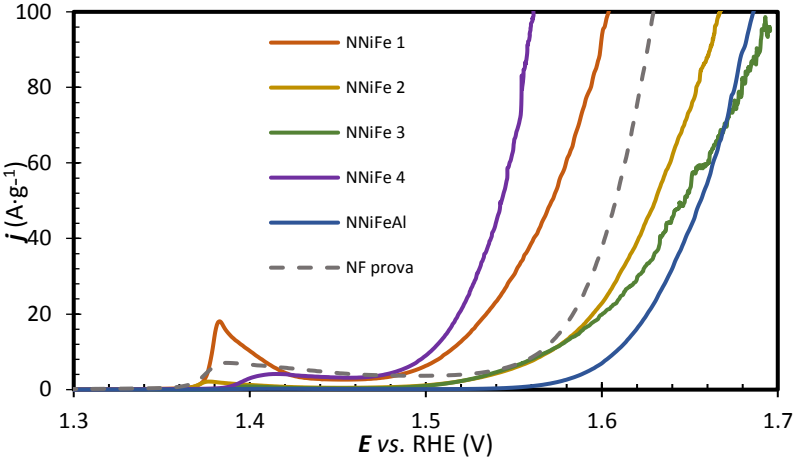

Figure 9.2. Polarization curves of ink deposition samples with at a scan rate of 2 mV·s^{-1}.

Table 8.2. Overpotential of ink deposition samples at 20 A·g^{-1}.

Sample	η_{20}(mV)	Sample	η_{20} (mV)
NNiFe 1	305±6	NNiFe 3	370±6
NNiFe 2	366±6	NNiFe 4	288±6
NNiFeAl	397±6	NF	354±6

The limiting steps given by the Tafel slopes in Figure 9.3 for NNiFe 1, 2 and NNiFeAl are the same possible for NiFeAl samples that being equations 3 and 5. Whereas NNiFe 3 and 4 have the same limiting steps as NiFe samples that being equation 2 and 4, but only equation 4 for NNiFe 3. From the ink deposition samples only NNiFe 4 has a similar overpotential and limiting step as the hydrothermal samples, meaning that the added Nafion177 interfere in the reaction.

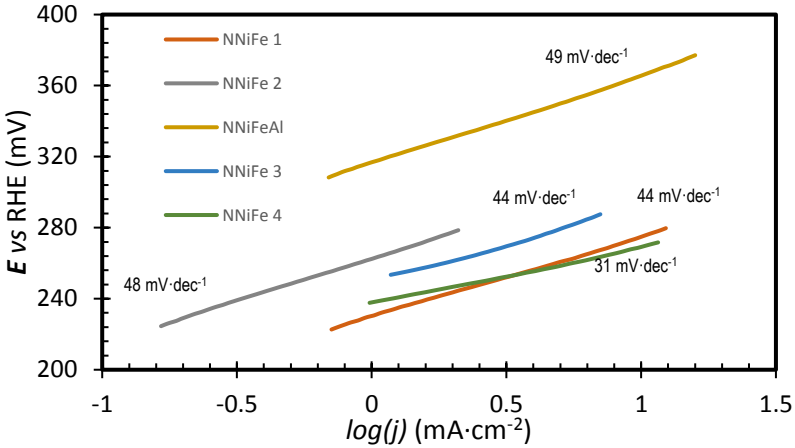

Figure 9.3. Tafel slopes for ink deposition samples.

10. CONCLUSIONS

After all the sample analysis we present the following conclusions.

The introduction of aluminium into the LDH structure results in an increase of the overpotential making the material a worse water splitting catalyst.

Both, the CHE and ECE treatments remove the aluminium of the sample at least partially.

For the anodic electrode of the water splitting reaction the best metal combination for the LDH is nickel and iron with an overpotential at 20 $A \cdot s^{-1}$ of 267 mV.

Both the CHE and ECE treatments does not improve the electrocatalytic performance of the material. On the one hand the CHE treatment does not have a big impact in the electrode performance, and its effects are unnoticeable in the electrochemical measures. On the other hand, the ECE treatment is much more effective to remove the aluminium from the samples but is not capable of making the material better than the non-aluminium counterparts.

The introduction of aluminium into the LDH does not change the material structure, and the following removal does not improve the catalytical properties of the LDH.

The limiting step of the reaction and how the LDH deposits depends on the metal combination of the LDH. For example, in the NiFe sample the Equation being 2 or 4.

The ink deposition method has the potential to work but needs more research.

11. REFERENCES AND NOTES

[1] C. Resini *et al.*, "Hydrogen production by ethanol steam reforming over Ni catalysts derived from hydrotalcite-like precursors: Catalyst characterization, catalytic activity and reaction path," *Appl. Catal. A Gen.*, vol. 355, no. 1–2, pp. 83–93, Feb. 2009, doi: 10.1016/j.apcata.2008.11.029.

[2] L. Feng *et al.*, "Nanoporous NiAl-LDH nanosheet arrays with optimized Ni active sites for efficient electrocatalytic alkaline water splitting," *Sustain. Energy Fuels*, vol. 4, no. 6, pp. 2850–2858, 2020, doi: 10.1039/D0SE00050G.

[3] T. Shinagawa, A. T. Garcia-Esparza, and K. Takanabe, "Insight on Tafel slopes from a microkinetic analysis of aqueous electrocatalysis for energy conversion," *Sci. Rep.*, vol. 5, no. 1, p. 13801, Nov. 2015, doi: 10.1038/srep13801.

[4] L. Li, K. S. Hui, K. N. Hui, Q. Xia, J. Fu, and Y.-R. Cho, "Facile synthesis of NiAl layered double hydroxide nanoplates for high-performance asymmetric supercapacitor," *J. Alloys Compd.*, vol. 721, pp. 803–812, Oct. 2017, doi: 10.1016/j.jallcom.2017.06.062.

[5] G. Mishra, B. Dash, and S. Pandey, "Layered double hydroxides: A brief review from fundamentals to application as evolving biomaterials," *Appl. Clay Sci.*, vol. 153, pp. 172–186, Mar. 2018, doi: 10.1016/j.clay.2017.12.021.

[6] H. Li, L. Zhang, S. Wang, and J. Yu, "Accelerated oxygen evolution kinetics on NiFeAl-layered double hydroxide electrocatalysts with defect sites prepared by electrodeposition," *Int. J. Hydrogen Energy*, vol. 44, no. 54, pp. 28556–28565, Nov. 2019, doi: 10.1016/j.ijhydene.2019.09.155.

[7] J. Wang *et al.*, "*In Situ* Ni/Al Layered Double Hydroxide and Its Electrochemical Capacitance Performance," *Energy & Fuels*, vol. 24, no. 12, pp. 6463–6467, Dec. 2010, doi: 10.1021/ef101150b.

[8] P. Benito, F. M. Labajos, and V. Rives, "Microwave-treated layered double hydroxides containing Ni2+ and Al3+: The effect of added Zn2+," *J. Solid State Chem.*, vol. 179, no. 12, pp. 3784–3797, Dec. 2006, doi: 10.1016/j.jssc.2006.08.010.

[9] M. S. Yarger, E. M. P. Steinmiller, and K.-S. Choi, "Electrochemical Synthesis of Zn−Al Layered Double Hydroxide (LDH) Films," *Inorg. Chem.*, vol. 47, no. 13, pp. 5859–5865, Jul. 2008, doi: 10.1021/ic800193j.

[10] H. Chen *et al.*, "Carbon-coated Hierarchical Ni–Mn Layered Double Hydroxide Nanoarrays on Ni Foam for Flexible High-capacitance Supercapacitors," *Electrochim. Acta*, vol. 213,

pp. 55–65, Sep. 2016, doi: 10.1016/j.electacta.2016.06.038.

[11] L.-J. Zhou, X. Huang, H. Chen, P. Jin, G.-D. Li, and X. Zou, “A high surface area flower-like Ni–Fe layered double hydroxide for electrocatalytic water oxidation reaction,” *Dalt. Trans.*, vol. 44, no. 25, pp. 11592–11600, 2015, doi: 10.1039/C5DT01474C.

[12] L. Zhang, K. N. Hui, K. San Hui, and H. Lee, “High-performance hybrid supercapacitor with 3D hierarchical porous flower-like layered double hydroxide grown on nickel foam as binder-free electrode,” *J. Power Sources*, vol. 318, pp. 76–85, Jun. 2016, doi: 10.1016/j.jpowsour.2016.04.010.

[13] B. Zhang *et al.*, “High-valence metals improve oxygen evolution reaction performance by modulating 3d metal oxidation cycle energetics,” *Nat. Catal.*, Oct. 2020, doi: 10.1038/s41929-020-00525-6.

[14] S.-L. Wang and P.-C. Wang, “In situ XRD and ATR-FTIR study on the molecular orientation of interlayer nitrate in Mg/Al-layered double hydroxides in water,” *Colloids Surfaces A Physicochem. Eng. Asp.*, vol. 292, no. 2–3, pp. 131–138, Jan. 2007, doi: 10.1016/j.colsurfa.2006.06.014.

[15] Mestres Pérez, Judith; Synthesis of layered double hydroxides by electrodeposition, Chemistry Final Projecte, University of Barcelona; January 2021.

12. ACRONYMS

ATR -> attenuated total reflection
CE -> counter electrode
CHE -> chemical etching
LDH -> layered double hydroxides
ECE -> electrochemical etching
EDX -> energy dispersive X-ray spectroscopy
HER -> hydrogen evolution reaction
NF -> nickel foam
OER -> oxygen evolution reaction
LSV -> linear sweep voltammetry
RHE -> reversible hydrogen electrode
SCE -> saturated calomel electrode
SEM -> scanning electron microscopy
WE -> working electrode
XRD -> X-ray diffraction